1   # Extrapolation Approaches for Creating

2   # Comprehensive Measurement-Based Methane

3   # Emissions Inventories

4   *Bailey K. Fosdick[1], Zachary Weller[1], Hon Xing Wong[1], Abigail Corbett[1], Yannik Roell[1], Ella*

5   *Martinez[1], Amanda Berry[1], Natalia Gielczowski[1], Kristian D. Hajny[1], Christopher Moore[1, *]*

6   [1] GTI Energy

7   [*]Christopher Moore – GTI Energy, 1700 S Mount Prospect Rd., Des Plaines, IL, 60018; Email:

8   cmoore@gti.energy

9

12   SYNOPSIS: We demonstrate statistically valid, practical extrapolation methods to develop

13   methane emissions inventories using measurements from a set of natural gas production assets.

## ABSTRACT

Measurement-based methane emissions inventories are essential for U.S. oil and natural gas operators to track their progress toward emissions targets, demonstrate the impact of improved operational and monitoring practices, and enable the scientific community to monitor methane budgets at various scales. However, translating raw emission measurement data, whether from continuous monitoring systems, aerial flyovers, or operational cause analyses, into emissions inventories is nontrivial, and advertised inventory numbers often lack any information about the methodology used to produce them. In this paper, we introduce the concept of a comprehensive measurement-based emissions inventory, which represents all emissions across the entire time frame, across all spatial assets, and of all emission sizes for the target scope. We carefully characterize some of the extrapolation efforts necessary to create a comprehensive emissions inventory estimate with data from either continuous monitoring systems or aerial flyover measurements. Understanding these methods is essential to create defensible emissions inventory reports that adhere to reporting frameworks such as Veritas and the Oil and Gas Methane Partnership 2.0. We provide simple examples to illustrate the sensitivity of annual emissions estimates to the various extrapolation approaches and highlight the challenges, strengths, and limitations when working with data from each of the technologies.

## 1. Introduction

Methane emissions from across the oil and natural gas supply chain are an important policy and climate topic, globally. Methane ($CH_4$), the primary component of natural gas, is a short-lived climate pollutant that has an $82.5 \pm 25.8$ times greater climate impact than carbon dioxide on a 20-year timeframe and $29.8 \pm 11$ on a 100-year timeframe.[1,2] Given the near-term impact of every kg

36    of $CH_4$ emitted, natural gas companies have an impetus to identify the largest sources of emissions

37    and to initiate mitigation strategies targeting these sources. The methane intensity (emissions per

38    production) of natural gas has also grown into a marketable quantity, as there is interest in gas

39    associated with lower overall emissions if it can be confidently determined.[3–5] The U.S.

40    Environmental Protection Agency's (EPA) Greenhouse Gas Reporting Program (GHGRP)

41    Subpart W is the current regulatory standard for reporting methane emissions from petroleum and

42    natural gas activities in the United States for covered facilities.[6]

43    Emission inventories are valuable tools that can be used to track and compare emissions,[7–9]

44    identify opportunities to limit pollution,[10,11] minimize wasted energy, and even save money.[12–14]

45    Inventories have traditionally been developed using Bottom-Up (BU) methods that combine broad,

46    generic emission factors with activity factors that estimate the frequency of emission events and

47    equipment/component/site counts (e.g., heaters, separators, blowdowns) to get a total emissions

48    estimate. The GHGRP regulations include the development of annual BU inventories at the facility

49    level, and the EPA Greenhouse Gas Inventory (GHGI) extends these data to estimate regional and

50    national totals. Emission inventories reported in the literature often focus on measurement-based,

51    or Top-Down (TD), approaches for large geographic areas such as a basin, state, or nation.[15–19] TD

52    studies have often shown emissions that are higher than estimated by the GHGI.[7,18–20] However,

53    other researchers have developed BU inventories that agree with these TD estimates and suggest

54    the GHGI underestimate stems from underestimating the impact of intermittent high-emission

55    events.[7,9,21,22] Generally, persistent emissions can be linked to leaks and design emissions, such as

56    pneumatic controllers and compression systems,[23] whereas intermittent sources can include

57    abnormal operating conditions like inefficient or unlit flares[23–26] and operational emissions such

58    as blowdowns and manual liquid unloadings.[23,27] While operators have begun documenting some

59 known emissions events, such as blowdowns, capturing accurate emissions data on unexpected

60 abnormal conditions remains a significant challenge.

61 TD methods rely on emissions measurement data collected over different spatial and temporal

62 scales from technologies with varying performance characteristics (e.g., probability of detection

63 (POD), site- vs component-level attribution).[28–31] For example, snapshot aerial surveys can

64 measure every active site during a campaign to provide full spatial coverage; however, they only

65 briefly measure each site. Conversely, point sensor networks (PSN), sometimes referred to as

66 continuous monitoring systems, detect and quantify site emissions continuously under acceptable

67 environmental conditions, yet they are frequently not deployed at all sites due to their cost.

68 Extrapolating the measurements from this monitored subset of sites to estimate emissions from

69 unmonitored sites can introduce significant uncertainty to the resulting inventory.[19,32] Furthermore,

70 both aerial surveys and PSNs are limited in their ability to detect small leaks based on their POD,

71 which depends on the methane quantification technology used, data collection characteristics (e.g.,

72 flying altitude, number of sensors), and wind conditions.

73 As a result of these considerations, a third type of emission inventory called a measurement-

74 informed inventory (MII) that integrates BU and TD data, leveraging the relative strengths of each

75 approach, has been the focus of recent literature.[10,15,33] Theoretically, such MIIs provide pathways

76 to obtaining a more accurate estimate of emissions and are the focus of several proposed

77 monitoring frameworks, such as Veritas,[34] higher levels of the MiQ gas certification program[35]

78 and the Oil and Gas Methane Partnership (OGMP) 2.0.[36] In this work, we discuss inventories using

79 the following terminology. A "measurement-based emissions inventory" relies solely on

80 measurement data and uses extrapolation procedures to obtain a total emissions estimate with the

81 desired temporal, spatial, and emissions ranges (e.g., for a subset of facilities or time). A

82    "comprehensive" emissions inventory is any inventory that completely reflects all temporal,

83    spatial, and emissions ranges for the target scope (e.g., annual total emissions for all facilities for

84    one operator).

85       The pathway to creating the most accurate MII involves reconciliation analyses that identify

86    reasons for the agreement or disagreement between different inventories, either TD and BU or

87    inventories relying on different emissions measurement information.[36–38] Such reconciliation is

88    only possible if the inventories are estimating the same quantity, meaning they have the same

89    spatiotemporal scope and estimate total emissions across that scope.[22,38–40] Both extrapolation and

90    reconciliation require analytical assumptions and rely on methodological decisions that can

91    significantly impact and bias the estimated emissions. However, there is currently no standardized

92    method. The differences in spatial, temporal, and emissions size coverage across measurement

93    technologies further complicate this situation.

94       Given the lack of standardization amid growing interest in MII development, this study aims to

95    document and demonstrate practical pathways for creating a comprehensive measurement-based

96    inventory. We propose multiple extrapolation methods, outline their underlying assumptions, and

97    discuss the variability across the resulting emissions estimates. To do so, we utilize anonymized

98    production data and emissions monitoring data from PSN and aerial surveys to develop two annual,

99    comprehensive measurement-based inventories for a dry gas basin. Though we demonstrate these

100   methods for a theoretical U.S. natural gas operator, the methods can be broadly applied, including

101   across other parts of the supply chain like transmission or distribution.

## 2. Materials and Methods

### 2.1. Extrapolation and Integration Considerations

We consider three data sources in this study: two PSN technologies (PSN A and PSN B) and one aerial survey method. These measurement technologies were originally deployed for leak detection and repair (LDAR) rather than for creating or informing emissions inventories, which introduces various critical nuances to the data that should be considered. While LDAR efforts are valuable in detecting and addressing leaks,[11,41–43] several studies have stressed the importance of representative sampling to develop appropriate MIIs,[15,32,40] and LDAR measurements may not collect a representative sample.

One LDAR aerial survey strategy is conducting an initial flight over all sites to detect emissions, followed by a second flight over only the sites with detected emissions to assess whether those emissions persist.[15,44,45] Developing a probabilistic model to account for the second flight's sampling bias is non-trivial and yet necessary to incorporate said data into an inventory estimate. For the purposes of this study, we focus solely on the first flight of each aerial campaign, as they represent spatially complete snapshot surveys of all facilities.

PSNs are thought to have excellent temporal resolution, while their spatial resolution is dependent on their level of deployment across sites. Spatial extrapolation is needed to estimate emissions for the sites without a PSN to create an emissions inventory. Temporal extrapolation is also necessary to infer emissions before the PSN installation and for periods when the environmental conditions were outside the operational envelope of the PSN.

Lastly, all technologies have detection limits. To develop a comprehensive inventory the dataset must be augmented with estimates of undetected emissions. Auxiliary information or assumptions about the emission size distribution, often referred to as the expected emissions distribution, are

125 required to do so. This augmentation may not be necessary if it can be demonstrated using an

126 expected emissions distribution that undetected emissions represent a minor contribution.

127 As shown in Figure 1, there are several steps to using emissions measurement data to create an

128 MII. The first step is to perform extrapolation of the monitoring data to develop a comprehensive

129 measurement-based inventory. For each technology and dimension (i.e., spatial, temporal,

130 emission size distribution), we detail several methods that vary in complexity. In this work, we

131 consider extrapolation methods that apply to a single dimension and then layer methods to obtain

132 a procedure that accounts for all necessary extrapolations. We begin by inferring undetected

133 emissions during monitoring times in Section 2.3. Next, we apply temporal extrapolation to get

134 annual estimates for monitored sites in Section 2.4. Finally, we apply spatial extrapolation to infer

135 emissions from unmonitored facilities in Section 2.5. Simple extrapolation approaches can be

136 useful when the assumptions are reasonable; however, often, more advanced extrapolation

137 methods will result in more accurate extrapolations, given systematic biases in the spatial and

138 temporal deployment of the technology. Nevertheless, any error in emission event frequency

139 estimation or emission quantification will translate through the extrapolation to error in the final

140 inventory. Thus, the emission rate quantification technology used fundamentally affects the quality

141 and uncertainty in any developed inventory.

142
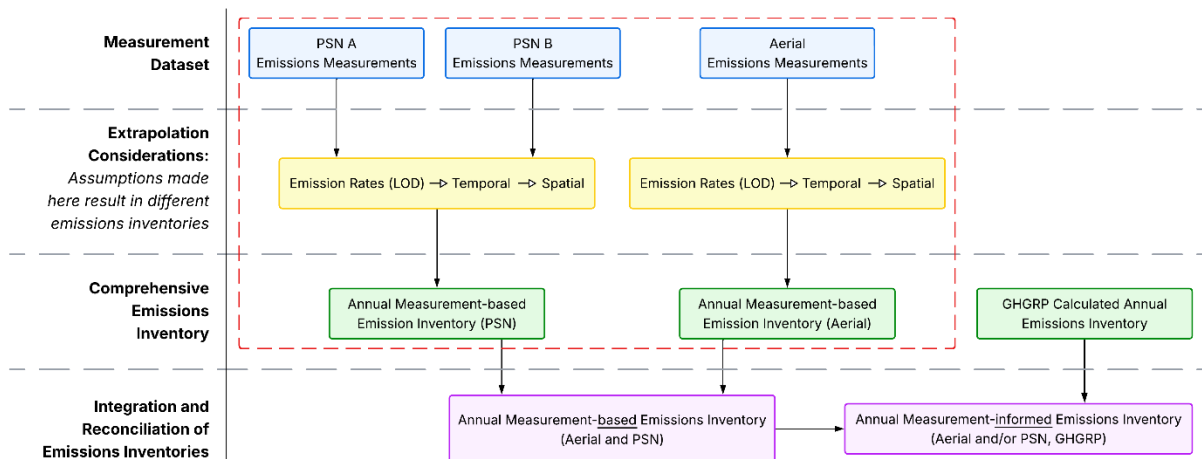
**Figure 1.** Flow diagram detailing all steps required to develop a measurement-informed emissions inventory. The focus of this work is highlighted in the red box.

The second step is integrating two or more of the developed emission inventories. This is where reconciliation occurs to produce an MII believed to provide the best representation of actual emissions. This can be as complex as the extrapolation.

## 2.2. Anonymized Dataset

This work uses anonymized production and emissions measurement data collected in 2023 from a dry-gas basin for a subset of sites shared by our operator partners. The anonymization is detailed in Supporting Information (SI) Text S1 and is intended to preserve important features and relationships in the data while making true values unrecoverable by a third party given the confidential nature of the data. A total of 200 anonymous sites were selected with all sites having been surveyed in two aerial surveys, 50 sites having PSN A, and 50 sites having PSN B. The aerial surveys use airborne Gas Mapping LiDAR (GML) to calculate emission rates[43,46] while the PSNs use one or more calibrated metal oxide CH4 sensors or tunable diode laser sensors and anemometers installed on-site to calculate an emission rate using proprietary formulae. Both PSNs

158 report emission rates as 15-minute averages, but PSN A reports 0 when no emissions are measured

159 and "NA" to indicate unable to calculate an emission rate while PSN B excludes both such times.

160 To make the PSN data sets more congruent and simplify the analysis of the PSN data, we randomly

161 replaced PSN B missing intervals with zero and NA, such that the ratio of zeroes relative to NA

162 matches that of PSN A (33%). This simplification treats the PSNs as though they have comparable

163 performance, which we note is not necessarily the case under real world conditions.[47] Figure 2

164 summarizes the relative coverage of each dataset along the various dimensions.

165
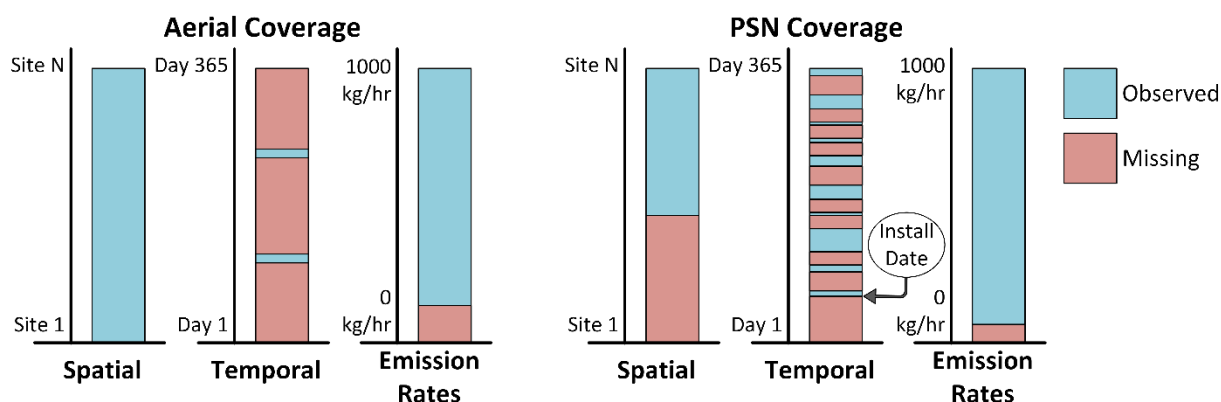


166 **Figure 2.** Qualitative diagrams showing the relative coverage of the aerial survey and the PSN

167 data across each dimension. The aerial survey data consists of two campaigns covering all sites

168 (Spring and Fall, 2023). Deployment of PSN on sites occurred throughout the year, creating an

169 additional unmonitored period for many sites at the beginning of the year.

## 2.3. Emission Rate Coverage

### 2.3.1. Aerial

172 Aerial surveys can scan many facilities relatively quickly, but their ability to detect emissions

173 depends on several factors, including sensor type, survey height, wind speed, and emission size.

174 Typically, there is a trade-off between spatial coverage and detection sensitivity, where flights

175 conducted at higher altitudes can scan facilities more quickly but at the expense of missing small

176 emissions. Several studies have examined the POD for human-piloted aircraft surveys.[28,46,48,49]

177 The aerial surveys in this work were conducted at relatively low altitudes to enable the attribution

178 of emissions to specific sources for the purposes of LDAR. This particular vendor has developed

179 methods to determine the POD using the emission rate and survey-specific information with a

180 typical 90% POD of 1.27 kg/h[46], however we are using the described production sector >90% POD

181 of 3 kg/h in this work.[43,50]

### 2.3.2. PSN

183 The two PSN technologies used in this work report slightly different detection capabilities.

184 Vendor listed performance specifications detail that PSN A can detect emission rates as low as 0.4

185 kg/h at distances up to 100 m, though this may represent a minimum detection threshold (POD >

186 0%) rather than an established 90% POD based on controlled release testing. PSN B has undergone

187 testing at the Methane Emissions Technology Evaluation Center (METEC) that determined a

188 minimum detection threshold of 0.12 kg/h and a 90% POD of 1.5 kg/h.[51]

### 2.3.3 Extrapolation Methods

190 For aerial survey data we consider a simple method to account for undetected emissions based

191 on the stated POD (see Table 1). For simplicity, our approach treats the >90% POD as a LOD

192 threshold assuming all emissions above are measured. We leverage the emission rate distribution

193 of Omara et al., [52] subset to only dry gas basins, to estimate the average emission rate and fraction

194 of emission rates below this LOD. Briefly, Omara et al.[52] combined site-level production sector

195 emissions data from previous studies with Enverus™ (Austin, TX USA) activity data using a

196 statistical resampling method to develop a national emission rate distribution. Note that other

197 national emission rate distribution estimates exist and could alternatively be used as the reference

198    distribution.[8,9] For comparison, we also consider the assumption that there are no emissions that

199    are undetected given the high sensitivity of the instruments used in this work.

200      In the Omara et al.[52] distribution, 24% of sites have emissions above a LOD of 3 kg/hr and 57%

201    have non-zero emissions below this LOD. We estimate the fraction of sites with undetected

202    emissions by assuming the 57% to 24% ratio is the same for our population of sites, and then

203    account for any observed measurements below the LOD. Mathematically, this estimate for the

204    proportion of undetected emissions can be expressed

205    $(0 < x < \text{LOD})_{undetected} = \left(\frac{0 < x < \text{LOD}}{> \text{LOD}}\right)_{Omara} \times (> \text{LOD})_{measured} - (< \text{LOD})_{measured}$    Eq. 1

206    We convert the percent of measurements calculated in Equation 1 to a number of measurements

207    and assign this number of non-emitting sites the average non-zero emission rate between 0 and 3

208    kg/h from Omara et al.[52], which is 0.922 kg/h.

209      Applying this approach using the PSN LOD and data resulted in negative corrections due to the

210    low LODs and many measured emission rates below the LOD. Therefore, no adjustments were

211    made to the PSN emission records to adjust for undetected emissions. If a different reference

212    distribution[8,9] were used, it is possible some correction may be warranted.

213    **Table 1.** Extrapolation approaches for inferring emissions below the LOD.

| Extrapolation Method | Description | Assumptions | Advantages/Disadvantages |
|---|---|---|---|
| 1. Assume all emissions are measured | Use data without modification | All emission rates are detectable by the technology | + Easy to implement<br><br>- Underestimates total emissions, particularly with less sensitive technology |
| 2. Augment observed emissions events with an additional undetected set of events based on fraction of literature expected emissions | Use literature emission rate distribution to estimate number of emissions | Literature emission rate distribution accurately reflects true | + Relatively easy to implement |

| distribution below technology LOD | events undetected | distribution of emissions on surveyed sites | + Directly accounts for small, missed emissions using best available data<br><br>- Simplistic approach that does not fully account for low emissions |
|---|---|---|---|

## 2.4. Temporal Extrapolation

### 2.4.1. Aerial

The aerial survey data are instantaneous snapshot measurements of the emissions from facilities. These observed emission rates must be extrapolated to all other times when the sites are unobserved. Since not all sites operate continuously throughout the year, three different extrapolation approaches were used.

In the first approach, aerial temporal method one (AT1), each observation is extrapolated across the year based on the number of observations at that site (i.e., two aerial emission observations would each be extrapolated over six months). While this extrapolation in essence assumes all sites with non-zero emissions emit constantly year-round, it is mathematically equivalent to computing the mean emission rate across all sites and assuming that is the true mean emission rate across all sites over the entire year. This extrapolation approach aligns with the ergodic hypothesis, which states that an average over the emissions measurements at many sites is equal to the time-averaged emissions at a single site, assuming sites are relatively homogeneous.[53]

In AT2, extrapolation accounts for site-specific production months, ensuring that emissions are only projected for the months that a site was actively producing. This method results in equal or lower estimated emissions compared to the first approach, though it may underestimate emissions since wells that are not active can still emit.[54–57] Note that no duration information is required here

232    as we assume that the relative frequency of the observed emissions reflects the frequency and

233    duration of the emission events.

234    In AT3, aggregated production-normalized emission rates are used in extrapolation rather than

235    scaling emissions at the individual site level. Specifically, total emissions observed during each

236    flyover are summed across sites, converted to monthly emission rates assuming 730 hours per

237    month, and divided by the total production from all sites during the corresponding month to get an

238    average emission intensity (i.e., emissions per unit of gas produced) for the month flown. The

239    intensities are then multiplied by the total production for each half of the year and summed. This

240    method assumes that emissions are proportionally related to production at the fleet level as

241    suggested by previous research,[52,58–60] though the relationship was weak, and accounts for

242    temporal fluctuations in production over time offering a broader, system-level estimate of total

243    emissions.

### 2.4.2. PSN

245    For many sites equipped with PSN, emission rate records are missing for large portions of the

246    year. There are two primary causes of the missing values: (1) unmonitored periods, often before

247    the PSN is installed on the site, and (2) periods of no information, when the PSN is actively

248    monitoring the site, but the environmental conditions prohibit emission rate estimation. Note that

249    the term "period of no information" used here is adopted from Daniels et al.[61] The portion of the

250    year designated as periods of no information varies significantly across PSN A sites (see SI Figure

251    S1), with an average of 61% of recorded time intervals (i.e., excluding unmonitored periods)

252    classified as periods of no information (range: 35% to 94%). In some cases, this includes large

253    windows (e.g., weeks to months) that are periods of no information. For context, Chen et al.,[62]

254 estimated via simulation that 78% of time would be periods of no-information with one sensor and

255 45% with four sensors for a single source emission event.

256    Table **2** outlines several approaches for temporally interpolating through periods of no

257 information, labeling these as PSN temporal methods (PT).

258 **Table 2**. Approaches for temporal extrapolation for missing emission rates from PSNs due to

259 periods of no information, listed in order of simplest to most complex.

| Extrapolation Method | Description | Assumptions | Advantages/Disadvantages |
|---|---|---|---|
| *PT1. Assume all missing emission rates are 0 | Set all missing emission rates during periods of no information to zero | No emissions occurred during time intervals when data is missing | + Easy to implement<br><br>- Likely underestimates emissions |
| PT2. Naïve scaling of total observed emissions by fraction of time emission rates were estimable (i.e., periods of information) | Calculate PSN total across all sites and multiply by a missing scaling factor (total interval count / intervals with emission rates reported). Equivalent to setting all periods of no information to the average measured emission rate across all sites with PSNs. | Data recorded is a representative sample of emissions across all PSN sites throughout the year | + Easy to implement<br><br>+ Wind is likely exogenous to cause of emissions so assumption of representativeness of sample is likely to hold<br><br>- Does not leverage temporally nearby emission rate information on either side of the missing window on a given site |
| PT3. Naïve scaling of site-level observed emissions by fraction of time the site emission rates were estimable (i.e., periods of information for the site) | Equivalent to method 2, but applied at the site level, rather than in aggregate. | Data recorded for the site is a representative sample of emissions for that site throughout the year | + Relatively easy to implement<br><br>+ Acknowledges possible site-to-site variability in total emissions<br><br>- Sites with very few reported emissions will have more variable scaling |

| Extrapolation Method | Description | Assumptions | Advantages/Disadvantages |
|---|---|---|---|
| PT4. Linear interpolation between emission rates on either side of missing window | Connect the emission rates during time windows just prior and just after period of no information. If the first or last time point is missing, extrapolate single observed rate through entire window. See SI Text S2 for more discussion. | Average emission rate in period of no information is well estimated by empirical average of observed endpoint emission rates. | + Leverages information on site at time periods surrounding period of no information<br><br>- Emission rates inferred are variable and if period of no information is large, method can extrapolate rare emission rate over large period |

260 *The first row is shaded red to highlight that it is not considered a valid approach to temporal
261 extrapolation but is included here for comparison purposes.

262     For unmonitored periods, we temporally extrapolate using a method analogous to AT2: multiply

263 the PSN total by a scaling factor that accounts for non-producing months (total months producing

264 / months monitored). This method was selected since unmonitored periods are typically months

265 long and is applied in an aggregate or site-specific manner to match the PSN temporal method.

## 2.5 Spatial Extrapolation

### 2.5.1. Aerial

268     The operator shares an updated site list with the aerial survey vendor a few weeks before each

269 flight to define the scope of the survey. Therefore, the survey provides 100% spatial coverage

270 across active sites, and no spatial extrapolation is required. This does not imply that all emissions

271 from every source are detected, but merely that all emission events, even those that are rare, are

272 within the sampling frame (e.g., leak from a tank, blowdown event, flare, vent). Hence, we assume

273 the observed emission rate distribution is representative of the true emission rate distribution.

### 2.5.2. PSN

275     Each of the approaches described here assumes that any necessary temporal extrapolation has

276 already been performed for the PSN data, and therefore, the key remaining extrapolation step is to

277    infer emissions at the sites without PSNs. To do this, it is critical to understand potential differences

278    between the characteristics of monitored and unmonitored sites. If site emissions are correlated

279    with site characteristics that exhibit notable differences between the groups of monitored and

280    unmonitored sites (i.e., newer sites, larger producing sites), extrapolation approaches ignoring

281    these site-level characteristics may result in biased emissions inventories.[15,19,32,40] For example,

282    Sherwin et al.[19] showed methane emission intensities that differed by more than a factor of two

283    across sub-basins within the Permian. This stresses the importance of appropriately considering

284    different types of facilities through stratification. We treat PSN A and PSN B data as a single PSN

285    dataset during spatial extrapolation. This assumes a site with PSN A is as well measured as PSN

286    B, which may not be true given different technology performance metrics (e.g., POD) and

287    algorithms used to convert measured concentrations into reported emission rates.

288      Figure 3 summarizes site characteristics for the monitored and unmonitored sites, partitioned by

289    technology provider with more details provided in SI Table S1. Most notably, the unmonitored

290    sites are older and have lower annual production. Focused on LDAR, the operator prioritized

291    installing PSNs on newer, high-production sites, as reflected in these statistics. Table 3 outlines

292    the three PSN spatial extrapolation methods (PS) considered here. Two of these methods consider

293    differences in facility characteristics, with PS2 stratifying facilities into inactive/no data, marginal

294    production (1 – 15 barrels of oil equivalent per day, BOED), standard production (16 – 300

295    BOED), and high production (>300 BOED) facilities.

296
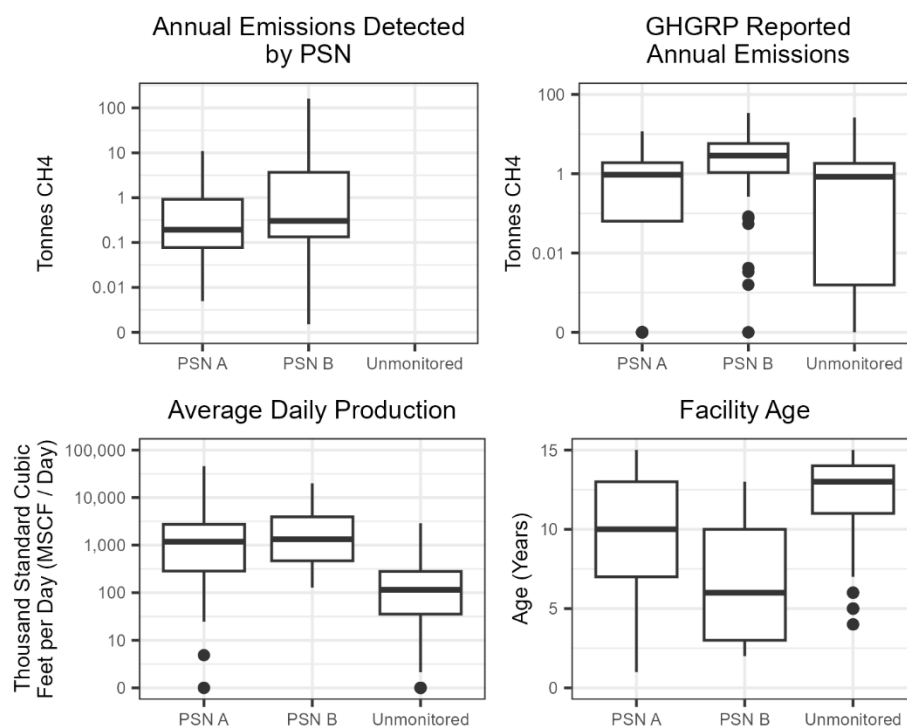
**Figure 3.** Distributions of site characteristics partitioned by whether it is equipped with PSN, and if so, what provider. Differences between monitored and unmonitored sites may be important to account for when creating a comprehensive measurement-based emissions inventory.

**Table 3.** Spatial extrapolation approaches for PSNs are listed in order of simplest to the most complex.

| Extrapolation Method | Description | Assumptions | Advantages/Disadvantages |
|---|---|---|---|
| PS1. Naïve scaling by the fraction of sites monitored | Calculate the total emissions from both PSN providers and multiply value by a site scaling factor (total site count / monitored sites) | Sites with PSN are a representative sample of all sites | + Easy to implement<br><br>- Figure 3 suggests the representative assumption may not be appropriate |
| PS2. Scaling by fraction of sites monitored within each | Compute total PSN emissions for each production strata and multiply by a strata- | Sites with PSN within each production strata are | + Easy to implement<br><br>+ Method can be replicated at basin-level since |

17

| production strata | specific site scaling factor (total site count in strata / monitored sites in strata), and sum across all strata | representative of all sites in the strata | production data is publicly available<br><br>- Figure 3 suggests the representative assumption may not be appropriate |
| PS3. Multivariable prediction model | Estimate multivariable regression model to predict total site emissions as detected by PSN as a function of site characteristics (age, production, GHGRP reported emissions) | Relationship between site characteristics and emissions on sites with PSN is the same for sites without PSN. | + More refined predictions of emissions at site level, which can account for biased placement of PSN on specific types of sites<br><br>- Implementation requires software that performs multivariable regression |

302

# 3. Results and Discussion

## 3.1. Applying Extrapolations to Aerial Surveys

305     The values in Table 4 show comprehensive measurement-based emissions inventories using the

306     aerial data. These results account for all three comprehensive inventory dimensions, using

307     temporal extrapolation and a <LOD correction. The LOD correction adds between 270 and 291

308     metric tons (MT) $CH_4$, depending on the method of temporal extrapolation, which equates to only

309     ~4.5% of the total. The choice of temporal extrapolation method also has little impact on the result.

310     Emissions including the LOD correction across temporal extrapolation methods differ by less than

311     5% relative to the average across all three methods (6,233 MT $CH_4$).

312     **Table 4.** Temporal extrapolation results for the aerial survey data for the monitored sites.

| Temporal Extrapolation Method | Temporally Extrapolated Inventory (MT $CH_4$) |
|---|---|
| AT1 – Assuming consistent emissions for 6 months from aerial measurement | 6153 |
| - Accounting for LOD | 6444 |

| | |
|---|---|
| AT2 – Account for production months | 5949 |
| - Accounting for LOD | 6219 |
| AT3 – Proportional scaling of production | 5764 |
| - Accounting for LOD | 6036 |

313  Our estimated contribution from undetected emissions is lower than reported by other recent

314  works. Previous studies have reported undetected emissions or emissions with 0% < POD < 100%

315  can represent as little as 5% to over 85% of total emissions depending on the basin.[15,19,43,45,63]

316  Given this large range, we cannot determine whether our ~4.5% estimate is low due to the study

317  area or methodology.

## 3.2. Applying PSN Temporal Extrapolations

319  In general, the linear interpolation and naïve scaling methods for PSN A (PT2 – PT4) all provide

320  similar results, whereas assuming all missing emission rates are zero (PT1) provides a substantially

321  smaller estimate (see Table 5). Table 5 first displays the extrapolation method results for periods

322  of no information and then includes the extrapolation method for unmonitored periods layered on

323  top. When accounting for unmonitored months, methods PT2 – PT4 differ by at most 11% relative

324  to the average across them (141 MT $CH_4$) while PT1 differs by 81% relative to 141 MT $CH_4$.

325  **Table 5.** Temporal extrapolation results for the PSN data for the monitored sites.

| Temporal Extrapolation Method for Periods of No Information | Partial Inventory (MT $CH_4$) | |
|---|---|---|
| | PSN A | PSN B |
| PT1. Assume all missing emission rates are 0 | 45 | 322 |
| - Accounting for unmonitored months | 60 | 474 |
| PT2. Naïve scaling of total observed emissions by fraction of time emission rates were estimable <br><br> - Accounting for unmonitored months | 118 <br><br> 155 | 734 <br><br> 1082 |

| | | |
|---|---|---|
| PT3. Naïve scaling of site-level observed emissions by fraction of time-specific site emission rates were estimable<br><br>- Accounting for unmonitored months | 98<br><br>127 | 513<br><br>540 |
| PT4. Linear interpolation between emission rates on either side of missing window<br><br>- Accounting for unmonitored months | 109<br><br>141 | 342<br><br>356 |

326    The results for PSN B are notably different than those for PSN A. First, partial inventory

327    emissions calculated using PSN B are higher on average than PSN A.  This is unsurprising given

328    the differences in the facilities being measured, as shown in Figure 3, though may also indicate

329    differences in performance between PSN A and PSN B. The fraction of unmonitored data is also

330    less consistent across sites for PSN B as compared to PSN A (see SI figure S2), with higher

331    emitting sites generally being more heavily monitored. This biased monitoring is likely why the

332    PT2-derived inventory is so much higher (~80%) than the average across PT1, PT3, and PT4 for

333    PSN B (457 MT $CH_4$), unlike what we see for PSN A. Additionally, more heavily sampling higher

334    emitters causes unmonitored periods to have a bigger impact if extrapolating aggregated data (PT1

335    and PT2), and a more minor impact if extrapolating site-level data (PT3 and PT4) as compared to

336    PSN A.

## 3.3. Applying PSN Spatial Extrapolations

338    There are substantial differences between the estimated inventories depending on the spatial

339    extrapolation approach, as shown in Table 6. Specifically, PS1 results are 1.8 times larger and PS2

340    results 1.2 times larger on average than those of PS3. All results presented have already been

341    temporally extrapolated, including accounting for unmonitored periods, such that they represent

342    annual estimates. As such, these results represent comprehensive measurement-based inventories

343    based on the PSN data. Results exclude PT1 as it was discussed that it is not considered a valid

344    approach, and PT2 is only included in PS1 as PT2 aggregates all sites before temporal

345    extrapolation and PS2 – PS3 can only be applied at the site level.

346    **Table 6.** Results from PSN spatial extrapolation methods.

| Spatial Extrapolation Method | Spatially Extrapolated Partial Inventory (MT CH$_4$) |
|---|---|
| PS1. Naïve scaling by the fraction of sites monitored | |
| - PT2 | 2474 |
| - PT3 | 1335 |
| - PT4 | 995 |
| PS2. Scaling by fraction of sites monitored within each production strata | |
| - PT3 | 849 |
| - PT4 | 668 |
| PS3. Multivariable prediction model | |
| - PT3 | 740 |
| - PT4 | 562 |

## 3.4 Comprehensive Emissions Inventory Estimates

348       Table 4 and Table 6 represent our comprehensive measurement-based inventory estimates for

349    aerial survey and PSN data, respectively. The aerial survey results range from 6,036 MT CH$_4$ to

350    6,444 MT CH$_4$ while the PSN results range from 562 MT CH$_4$ to 2,474 MT CH$_4$, even though the

351    spatio-temporal scope of each inventory is the same. We discuss this discrepancy in Section 3.5.

352    For both measurement systems, the method choice for temporal extrapolation had a minimal

353    impact on the emission estimate. The exceptions being PT1, which will always be biased low, and

354    PT2, which can be biased if some types of sites have more data than others. Spatial extrapolation

355     methods for PSN showed more variability across methods. For both measurement systems, we

356     also generally see that the more complex the extrapolation approach, excluding PT1, the lower the

357     estimated emission rate (i.e., AT3 < AT2, PS3 < PS2, etc.). This result may not be generalizable

358     and could look different if other extrapolation methods were considered.

## 3.5. Limitations

360     Since the amount of time the sites are monitored with the aerial survey is so limited, the annual

361     emissions inventories based on the temporal extrapolations will vary greatly depending on the

362     distribution of emission rates seen on the survey. Specifically, a modeling study estimated naïve

363     scaling of semi-annual measurements would result in an average of between 18% and 48%

364     sampling error, depending on the duration of intermittent events.[64] It is also possible PSN may

365     miss or underestimate certain sources that aerial surveys capture. The potential underestimation of

366     ground-based measurements was discussed in depth in SI Section S1.2 of Sherwin et al.[19] PSN

367     controlled release studies with large emission rates and in real-world settings have also reported

368     emission size quantification underestimation of ~75% on average across several PSN.[47,65] Standard

369     controlled release studies show the majority of estimates are within a factor of three of true

370     emissions, though individual estimates can be biased low or high by over a factor of ten.[29,51,66]

371     Importantly, these standard controlled release studies have also shown a gradual improvement in

372     PSN performance over successive studies.

373     Contemporaneous comparisons of aerial survey and PSN data may clarify potential causes for

374     any differences between the two, especially if available at the source level where supervisory

375     control and data acquisition (SCADA) can also be compared.[10] However, this type of

376     reconciliation and cause analysis work is beyond the scope of this work. SCADA and/or PSN data

377     could also be used to inform more complex, but more appropriate methods of temporally scaling

378    aerial survey data that accounts for intermittent events, while aerial surveys can provide an

379    independent point of comparison for PSN. This has been discussed as a necessary next step to best

380    utilize these complementary measurement techniques in several recent works.[10,40,61,64] However,

381    direct reconciliation between these measurements is not feasible at the annual scale as presented

382    here.

## 3.6. Challenges in Aligning with Operational Realities

384    The emissions monitoring and survey measurements were collected as part of ongoing operator

385    LDAR efforts rather than the development of an MII. As a result, key decisions were driven by

386    different priorities. These design choices, such as the aerial survey strategy of revisiting emitting

387    sites, produce analytical challenges and limitations for estimating comprehensive emission

388    inventories. Fundamentally, the data collected from aerial surveys and PSN technologies do not

389    have complete coverage spatially, temporally, and across the emissions rate distribution, and

390    therefore, extrapolation is necessary to obtain an estimate of annual emissions. Importantly, such

391    a challenge is likely to exist across operators prioritizing LDAR and treating the creation of an MII

392    as a secondary benefit.

393    Current protocols and guidelines, such as Veritas,[34] OGMP 2.0,[36] and MiQ[35] provide insufficient

394    guidance for operators concerning the extrapolation methodologies needed to develop an MII,

395    particularly given the likelihood that data was not collected specifically to develop an MII. The

396    representativeness and accuracy of an emissions inventory are a function of how comprehensively

397    the data covers the relevant dimensions and the analytical methods used to process the data. With

398    the current state of monitoring technologies, extrapolation methods are necessary to develop a

399    credible, comprehensive inventory from measurement data. While advanced extrapolation

400    methods often result in the most accurate estimates, operators lack guidance on the impact of

401 various extrapolation methods on resulting MIIs and the tools and best practices to implement

402 more accurate extrapolation methods. As such, operators must make assumptions regarding the

403 emissions, and different assumptions will lead them to different extrapolation methods. This work

404 begins to address these gaps and shows how these different underlying assumptions can impact

405 the estimated emissions.

## 3.7. Implications and Future work

407 Interpreting estimates of emissions inventories and comparing estimates across basins or over

408 time is difficult without uncertainty estimates provided alongside the point estimates. Accurately

409 quantifying uncertainty in the measurement-based inventories outlined here will be the focus of

410 future research. Two key learnings from this work are (1) that the choice of extrapolation method

411 can greatly impact inventory estimates and therefore careful consideration of assumptions

412 underlying these methods is warranted, and (2) there are significant barriers to performing

413 reconciliation between some monitoring technologies and calculated inventories at the source level

414 (e.g., between PSN and Subpart W). While this work is based on a single dataset from a single

415 operator, these key learnings are generalizable to the development of an MII for any spatial and

416 temporal scope, given they are rooted in the underlying assumptions and mathematics associated

417 with different extrapolation methods. The extrapolation methods presented here were applied to

418 one dimension of coverage at a time (e.g. spatial, temporal, or emissions size), and therefore, they

419 needed to be layered to arrive at a comprehensive emissions inventory. More advanced statistical

420 methods could be constructed to perform extrapolation simultaneously across multiple

421 dimensions. Such methods would be able to more accurately model individual site emission

422 profiles and capture temporal correlation from one year to the next. This is an area of future work.

## Notes

The authors declare no competing financial interest.

## Supporting Information

The following files are available free of charge.

A full description of the methods used to anonymize the datasets used in this work (Text S1); A brief description of an alternative method used for linear temporal extrapolation of PSN data in cases without a measured endpoint (Text S2); Histogram of the percentage of time periods for PSN A that are periods of no information (Figure S1); Percentage of time periods for PSN that are unmonitored and periods of no information by site (Figure S2); visualization of the PSN A temporal extrapolation methods (Figure S2); detailed breakdown of all variables used in the multivariable prediction model used in the PSN spatial extrapolation partitioned by vendor and unmonitored periods (Table S1) (PDF).

Anonymized data and processing code is available through GitHub (https://github.com/yroell-gti/operator_mii_extrapolations).

## Abbreviations

$CH_4$, methane; EPA, Environmental Protection Agency; GHGRP, Greenhouse Gas Reporting Program; GHGI, Greenhouse Gas Inventory; BU, bottom-up; TD, top-down; POD, probability of detection; PSN, Point Sensor Networks; LOD, limit of detection; SI, Supporting Information; GML, Gas Mapping LiDAR; MII, measurement-informed inventory; OGMP, Oil and Gas Methane Partnership; LDAR, leak detection and repair; MT, metric ton; AT, aerial survey temporal extrapolation method; PT, point sensor network temporal extrapolation method; PS,

444    point sensor network spatial extrapolation method; BOED, barrels of oil equivalent per day;

445    SCADA, supervisory control and data acquisition.

## Acknowledgments

449

450

# 4. References

(1)     Abernethy, S.; Jackson, R. B. Global Temperature Goals Should Determine the Time Horizons for Greenhouse Gas Emission Metrics. *Environ. Res. Lett.* **2022**, *17* (2), 024019. https://doi.org/10.1088/1748-9326/ac4940.

(2)     Forster, P.; Storelvmo, T.; Armour, K.; Collins, W.; Dufresne, J.-L.; Frame, D.; Lunt, D. J.; Mauritsen, T.; Palmer, M. D.; Watanabe, M.; Wild, M.; Zhang, H. The Earth's Energy Budget, Climate Feedbacks, and Climate Sensitivity. In *Climate Change 2021: The Physical Science Basis. Contribution of Working Group I to the Sixth Assessment Report of the Intergovernmental Panel on Climate Change*; Masson-Delmotte, V., Zhai, P., Pirani, A., Connors, S. L., Péan, C., Berger, S., Caud, N., Chen, Y., Goldfarb, L., Gomis, M. I., Huang, M., Leitzell, K., Lonnoy, E., Matthews, J. B. R., Maycock, T. K., Waterfield, T., Yelekçi, O., Yu, R., Zhou, B., Eds.; Cambridge University Press, Cambridge, United Kingdom and New York, NY, USA, 2021; pp 923–1054.

(3)     Garg, S.; Boz, D. E.; Gilbert, B.; Crompton, J. A Critical Review of Natural Gas Emissions Certification in the United States. *Environ. Res. Lett.* **2023**, *18* (2), 023002. https://doi.org/10.1088/1748-9326/acb4af.

(4)     Handler, B.; Ayaburi, F. The Cleaning of U.S. Natural Gas; Evolution of Differentiated Gas and Related Crediting Mechanisms. *Resources Policy* **2024**, *90*, 104750. https://doi.org/10.1016/j.resourpol.2024.104750.

(5)     Ravikumar, A. P.; Tullos, E. E.; Allen, D. T.; Cahill, B.; Hamburg, S. P.; Zimmerle, D.; Fox, T. A.; Caltagirone, M.; Owens, L.; Stout, R.; Grimes, A. J.; Fernandez, T. M.; Jenks, C.; Duren, R.; Halff, A.; Bazilian, M. D.; Rucker, S. Measurement-Based Differentiation of Low-Emission Global Natural Gas Supply Chains. *Nat Energy* **2023**, *8* (11), 1174–1176. https://doi.org/10.1038/s41560-023-01381-x.

(6)     Electronic Code of Federal Regulations. *40 Code of Federal Regulations §98.230 - 98.238*; 2010. https://www.ecfr.gov/current/title-40/part-98/subpart-W (accessed 2025-04-08).

(7)     Alvarez, R. A.; Zavala-Araiza, D.; Lyon, D. R.; Allen, D. T.; Barkley, Z. R.; Brandt, A. R.; Davis, K. J.; Herndon, S. C.; Jacob, D. J.; Karion, A.; Kort, E. A.; Lamb, B. K.; Lauvaux, T.; Maasakkers, J. D.; Marchese, A. J.; Omara, M.; Pacala, S. W.; Peischl, J.; Robinson, A. L.; Shepson, P. B.; Sweeney, C.; Townsend-Small, A.; Wofsy, S. C.; Hamburg, S. P. Assessment of Methane Emissions from the U.S. Oil and Gas Supply Chain. *Science* **2018**, *361* (6398), 186–188. https://doi.org/10.1126/science.aar7204.

(8)     Omara, M.; Himmelberger, A.; MacKay, K.; Williams, J. P.; Benmergui, J.; Sargent, M.; Wofsy, S. C.; Gautam, R. Constructing a Measurement-Based Spatially Explicit Inventory of US Oil and Gas Methane Emissions (2021). *Earth System Science Data* **2024**, *16* (9), 3973–3991. https://doi.org/10.5194/essd-16-3973-2024.

(9)     Rutherford, J. S.; Sherwin, E. D.; Ravikumar, A. P.; Heath, G. A.; Englander, J.; Cooley, D.; Lyon, D.; Omara, M.; Langfitt, Q.; Brandt, A. R. Closing the Methane Gap in US Oil and Natural Gas Production Emissions Inventories. *Nat Commun* **2021**, *12* (1), 4715. https://doi.org/10.1038/s41467-021-25017-4.

(10)   Daniels, W. S.; Wang, J. L.; Ravikumar, A. P.; Harrison, M.; Roman-White, S. A.; George, F. C.; Hammerling, D. M. Toward Multiscale Measurement-Informed Methane Inventories: Reconciling Bottom-Up Site-Level Inventories with Top-Down Measurements Using Continuous Monitoring Systems. *Environ. Sci. Technol.* **2023**, *57* (32), 11823–11833. https://doi.org/10.1021/acs.est.3c01121.

(11)   Wang, J. L.; Barlow, B.; Funk, W.; Robinson, C.; Brandt, A.; Ravikumar, A. P. Large-Scale Controlled Experiment Demonstrates Effectiveness of Methane Leak Detection and Repair Programs at Oil and Gas Facilities. *Environ. Sci. Technol.* **2024**, *58* (7), 3194–3204. https://doi.org/10.1021/acs.est.3c09147.

(12) Johnson, F.; Wlazlo, A.; Keys, R.; Desai, V.; Wetherley, E. B.; Calvert, R.; Berman, E. S. F. Airborne Methane Surveys Pay for Themselves: An Economic Case Study of Increased Revenue from Emissions Control. EarthArXiv July 15, 2021. https://eartharxiv.org/repository/view/2532/ (accessed 2025-04-15).

(13) Kemp, C. E.; Ravikumar, A. P. New Technologies Can Cost Effectively Reduce Oil and Gas Methane Emissions, but Policies Will Require Careful Design to Establish Mitigation Equivalence. *Environ. Sci. Technol.* **2021**, *55* (13), 9140–9149. https://doi.org/10.1021/acs.est.1c03071.

(14) Schwietzke, S.; Harrison ,Matthew; Lauderdale ,Terri; Branson ,Ken; Conley ,Stephen; George ,Fiji C.; Jordan ,Doug; Jersey ,Gilbert R.; Zhang ,Changyong; Mairs ,Heide L.; Pétron ,Gabrielle; and Schnell, R. C. Aerially Guided Leak Detection and Repair: A Pilot Field Study for Evaluating the Potential of Methane Emission Detection and Cost-Effectiveness. *Journal of the Air & Waste Management Association* **2019**, *69* (1), 71–88. https://doi.org/10.1080/10962247.2018.1515123.

(15) Johnson, M. R.; Conrad, B. M.; Tyner, D. R. Creating Measurement-Based Oil and Gas Sector Methane Inventories Using Source-Resolved Aerial Surveys. *Commun Earth Environ* **2023**, *4* (1), 1–9. https://doi.org/10.1038/s43247-023-00769-7.

(16) Peischl, J.; Ryerson, T. B.; Aikin, K. C.; de Gouw, J. A.; Gilman, J. B.; Holloway, J. S.; Lerner, B. M.; Nadkarni, R.; Neuman, J. A.; Nowak, J. B.; Trainer, M.; Warneke, C.; Parrish, D. D. Quantifying Atmospheric Methane Emissions from the Haynesville, Fayetteville, and Northeastern Marcellus Shale Gas Production Regions. *Journal of Geophysical Research: Atmospheres* **2015**, *120* (5), 2119–2139. https://doi.org/10.1002/2014JD022697.

(17) Peischl, J.; Karion, A.; Sweeney, C.; Kort, E. A.; Smith, M. L.; Brandt, A. R.; Yeskoo, T.; Aikin, K. C.; Conley, S. A.; Gvakharia, A.; Trainer, M.; Wolter, S.; Ryerson, T. B. Quantifying Atmospheric Methane Emissions from Oil and Natural Gas Production in the Bakken Shale Region of North Dakota. *Journal of Geophysical Research: Atmospheres* **2016**, *121* (10), 6101–6111. https://doi.org/10.1002/2015JD024631.

(18) Shen, L.; Gautam, R.; Omara, M.; Zavala-Araiza, D.; Maasakkers, J. D.; Scarpelli, T. R.; Lorente, A.; Lyon, D.; Sheng, J.; Varon, D. J.; Nesser, H.; Qu, Z.; Lu, X.; Sulprizio, M. P.; Hamburg, S. P.; Jacob, D. J. Satellite Quantification of Oil and Natural Gas Methane Emissions in the US and Canada Including Contributions from Individual Basins. *Atmospheric Chemistry and Physics* **2022**, *22* (17), 11203–11215. https://doi.org/10.5194/acp-22-11203-2022.

(19) Sherwin, E. D.; Rutherford, J. S.; Zhang, Z.; Chen, Y.; Wetherley, E. B.; Yakovlev, P. V.; Berman, E. S. F.; Jones, B. B.; Cusworth, D. H.; Thorpe, A. K.; Ayasse, A. K.; Duren, R. M.; Brandt, A. R. US Oil and Gas System Emissions from Nearly One Million Aerial Site Measurements. *Nature* **2024**, *627* (8003), 328–334. https://doi.org/10.1038/s41586-024-07117-5.

(20) Brandt, A. R.; Heath, G. A.; Kort, E. A.; O'Sullivan, F.; Pétron, G.; Jordaan, S. M.; Tans, P.; Wilcox, J.; Gopstein, A. M.; Arent, D.; Wofsy, S.; Brown, N. J.; Bradley, R.; Stucky, G. D.; Eardley, D.; Harriss, R. Methane Leaks from North American Natural Gas Systems. *Science* **2014**, *343* (6172), 733–735. https://doi.org/10.1126/science.1247045.

(21) Lyon, D. R.; Zavala-Araiza, D.; Alvarez, R. A.; Harriss, R.; Palacios, V.; Lan, X.; Talbot, R.; Lavoie, T.; Shepson, P.; Yacovitch, T. I.; Herndon, S. C.; Marchese, A. J.; Zimmerle, D.; Robinson, A. L.; Hamburg, S. P. Constructing a Spatially Resolved Methane Emission Inventory for the Barnett Shale Region. *Environ. Sci. Technol.* **2015**, *49* (13), 8147–8157. https://doi.org/10.1021/es506359c.

(22) Zavala-Araiza, D.; Lyon, D. R.; Alvarez, R. A.; Davis, K. J.; Harriss, R.; Herndon, S. C.; Karion, A.; Kort, E. A.; Lamb, B. K.; Lan, X.; Marchese, A. J.; Pacala, S. W.; Robinson, A. L.; Shepson, P. B.; Sweeney, C.; Talbot, R.; Townsend-Small, A.; Yacovitch, T. I.; Zimmerle, D. J.; Hamburg, S. P. Reconciling Divergent Estimates of Oil and Gas Methane Emissions. *Proceedings of the National Academy of Sciences* **2015**, *112* (51), 15597–15602. https://doi.org/10.1073/pnas.1522126112.

(23) Zavala-Araiza, D.; Alvarez, R. A.; Lyon, D. R.; Allen, D. T.; Marchese, A. J.; Zimmerle, D. J.; Hamburg, S. P. Super-Emitters in Natural Gas Infrastructure Are Caused by Abnormal Process Conditions. *Nat Commun* **2017**, *8* (1), 14012. https://doi.org/10.1038/ncomms14012.

(24) Gvakharia, A.; Kort, E. A.; Brandt, A.; Peischl, J.; Ryerson, T. B.; Schwarz, J. P.; Smith, M. L.; Sweeney, C. Methane, Black Carbon, and Ethane Emissions from Natural Gas Flares in the Bakken Shale, North Dakota. *Environ. Sci. Technol.* **2017**, *51* (9), 5317–5325. https://doi.org/10.1021/acs.est.6b05183.

(25) Irakulis-Loitxate, I.; Guanter, L.; Liu, Y.-N.; Varon, D. J.; Maasakkers, J. D.; Zhang, Y.; Chulakadabba, A.; Wofsy, S. C.; Thorpe, A. K.; Duren, R. M.; Frankenberg, C.; Lyon, D. R.; Hmiel, B.; Cusworth, D. H.; Zhang, Y.; Segl, K.; Gorroño, J.; Sánchez-García, E.; Sulprizio, M. P.; Cao, K.; Zhu, H.; Liang, J.; Li, X.; Aben, I.; Jacob, D. J. Satellite-Based Survey of Extreme Methane Emissions in the Permian Basin. *Science Advances* **2021**, *7* (27), eabf4507. https://doi.org/10.1126/sciadv.abf4507.

(26) Plant, G.; Kort, E. A.; Brandt, A. R.; Chen, Y.; Fordice, G.; Gorchov Negron, A. M.; Schwietzke, S.; Smith, M.; Zavala-Araiza, D. Inefficient and Unlit Natural Gas Flares Both Emit Large Quantities of Methane. *Science* **2022**, *377* (6614), 1566–1571. https://doi.org/10.1126/science.abq0385.

(27) Allen, D. T.; Sullivan, D. W.; Zavala-Araiza, D.; Pacsi, A. P.; Harrison, M.; Keen, K.; Fraser, M. P.; Daniel Hill, A.; Lamb, B. K.; Sawyer, R. F.; Seinfeld, J. H. Methane Emissions from Process Equipment at Natural Gas Production Sites in the United States: Liquid Unloadings. *Environ. Sci. Technol.* **2015**, *49* (1), 641–648. https://doi.org/10.1021/es504016r.

(28) El Abbadi, S. H.; Chen, Z.; Burdeau, P. M.; Rutherford, J. S.; Chen, Y.; Zhang, Z.; Sherwin, E. D.; Brandt, A. R. Technological Maturity of Aircraft-Based Methane Sensing for Greenhouse Gas Mitigation. *Environ. Sci. Technol.* **2024**, *58* (22), 9591–9600. https://doi.org/10.1021/acs.est.4c02439.

(29) Ilonze, C.; Emerson, E.; Duggan, A.; Zimmerle, D. Assessing the Progress of the Performance of Continuous Monitoring Solutions under a Single-Blind Controlled Testing Protocol. *Environ. Sci. Technol.* **2024**, *58* (25), 10941–10955. https://doi.org/10.1021/acs.est.3c08511.

(30) Brown, J. A.; Harrison, M. R.; Rufael, T.; Roman-White, S. A.; Ross, G. B.; George, F. C.; Zimmerle, D. Informing Methane Emissions Inventories Using Facility Aerial Measurements at Midstream Natural Gas Facilities. *Environ. Sci. Technol.* **2023**, *57* (39), 14539–14547. https://doi.org/10.1021/acs.est.3c01321.

(31) Daniels, W. S.; Kidd, S. G.; Yang, S. L.; Stokes, S.; Ravikumar, A. P.; Hammerling, D. M. Intercomparison of Three Continuous Monitoring Systems on Operating Oil and Gas Sites. *ACS EST Air* **2025**, *2* (4), 564–577. https://doi.org/10.1021/acsestair.4c00298.

(32) Schissel, C.; Allen, D.; Dieter, H. Methods for Spatial Extrapolation of Methane Measurements in Constructing Regional Estimates from Sample Populations. *Environ. Sci. Technol.* **2024**, *58* (6), 2739–2749. https://doi.org/10.1021/acs.est.3c08185.

(33) Ravikumar, A. P.; Li, H.; Yang, S. L.; Smith, M. L. Developing Measurement-Informed Methane Emissions Inventory Estimates at Midstream Compressor Stations. *ACS EST Air* **2025**, *2* (3), 358–367. https://doi.org/10.1021/acsestair.4c00237.

(34) GTI Energy. *Veritas*. https://veritas.gti.energy/ (accessed 2025-04-09).

(35) MiQ. *MiQ is the fastest growing and most trusted methane emissions certification standard*. https://miq.org/ (accessed 2025-04-09).

(36) United Nations Environment Programme. *OGMP 2.0 Reconciliation and Uncertainty Guidance*; 2022. https://www.ogmpartnership.org/ (accessed 2024-12-20).

(37) Fox, T. *What is Emissions Reconciliation?*. Highwood Emissions Management. https://highwoodemissions.com/bulletin/what-is-emissions-reconciliation/ (accessed 2025-04-08).

(38) Vaughn, T. L.; Bell, C. S.; Pickering, C. K.; Schwietzke, S.; Heath, G. A.; Pétron, G.; Zimmerle, D. J.; Schnell, R. C.; Nummedal, D. Temporal Variability Largely Explains Top-down/Bottom-up Difference

593      in Methane Emission Estimates from a Natural Gas Production Region. *Proceedings of the National*
594      *Academy of Sciences* **2018**, *115* (46), 11712–11717. https://doi.org/10.1073/pnas.1805687115.

595 (39) Chen, Y.; Sherwin, E. D.; Wetherley, E. B.; Yakovlev, P. V.; Berman, E. S. F.; Jones, B. B.; Hmiel, B.;
596      Lyon, D. R.; Duren, R.; Cusworth, D. H.; Brandt, A. R. Reconciling Ultra-Emitter Detections from Two
597      Aerial Hyperspectral Imaging Surveys in the Permian Basin. EarthArXiv March 16, 2024.
598      https://eartharxiv.org/repository/view/6860/ (accessed 2025-04-15).

599 (40) Wang, J. L.; Daniels, W. S.; Hammerling, D. M.; Harrison, M.; Burmaster, K.; George, F. C.;
600      Ravikumar, A. P. Multiscale Methane Measurements at Oil and Gas Facilities Reveal Necessary
601      Frameworks for Improved Emissions Accounting. *Environ. Sci. Technol.* **2022**, *56* (20), 14743–14752.
602      https://doi.org/10.1021/acs.est.2c06211.

603 (41) Cheadle, L. C.; Tran, T.; Nyarady, J. F.; Lozo, C. Leak Detection and Repair Data from California's Oil
604      and Gas Methane Regulation Show Decrease in Leaks over Two Years. *Environmental Challenges*
605      **2022**, *8*, 100563. https://doi.org/10.1016/j.envc.2022.100563.

606 (42) Ravikumar, A. P.; Roda-Stuart, D.; Liu, R.; Bradley, A.; Bergerson, J.; Nie, Y.; Zhang, S.; Bi, X.; Brandt,
607      A. R. Repeated Leak Detection and Repair Surveys Reduce Methane Emissions over Scale of Years.
608      *Environ. Res. Lett.* **2020**, *15* (3), 034029. https://doi.org/10.1088/1748-9326/ab6ae1.

609 (43) Thorpe, M. J.; Donahue, C. P.; Kreitinger, A.; Roos, P. A.; Brasseur, J. K.; Losby, B.; Greenfield, N.;
610      Carre-Burritt, A.; Kunkel, W. M.; Altamura, D. T.; Dudiak, C. D.; Oberoi, K.; Hengst, V. Total Emissions
611      Estimation for Oil and Gas Production Facilities Using Aerial Gas Mapping LiDAR; 2024; p
612      D011S015R002. https://doi.org/10.2118/222020-MS.

613 (44) Johnson, M. R.; Tyner, D. R.; Conrad, B. M. Origins of Oil and Gas Sector Methane Emissions: On-
614      Site Investigations of Aerial Measured Sources. *Environ. Sci. Technol.* **2023**, *57* (6), 2484–2494.
615      https://doi.org/10.1021/acs.est.2c07318.

616 (45) Conrad, B. M.; Tyner, D. R.; Li, H. Z.; Xie, D.; Johnson, M. R. A Measurement-Based Upstream Oil
617      and Gas Methane Inventory for Alberta, Canada Reveals Higher Emissions and Different Sources
618      than Official Estimates. *Commun Earth Environ* **2023**, *4* (1), 1–10. https://doi.org/10.1038/s43247-
619      023-01081-0.

620 (46) Thorpe, M. J.; Kreitinger, A.; Altamura, D. T.; Dudiak, C. D.; Conrad, B. M.; Tyner, D. R.; Johnson, M.
621      R.; Brasseur, J. K.; Roos, P. A.; Kunkel, W. M.; Carre-Burritt, A.; Abate, J.; Price, T.; Yaralian, D.;
622      Kennedy, B.; Newton, E.; Rodriguez, E.; Elfar, O. I.; Zimmerle, D. J. Deployment-Invariant Probability
623      of Detection Characterization for Aerial LiDAR Methane Detection. *Remote Sensing of Environment*
624      **2024**, *315*, 114435. https://doi.org/10.1016/j.rse.2024.114435.

625 (47) Chen, Z.; El Abbadi, S. H.; Sherwin, E. D.; Burdeau, P. M.; Rutherford, J. S.; Chen, Y.; Zhang, Z.;
626      Brandt, A. R. Comparing Continuous Methane Monitoring Technologies for High-Volume Emissions:
627      A Single-Blind Controlled Release Study. *ACS EST Air* **2024**, *1* (8), 871–884.
628      https://doi.org/10.1021/acsestair.4c00015.

629 (48) Bell, C. S.; Rutherford, J.; Brandt, A.; Sherwin, E.; Vaughn, T.; Zimmerle, D. Single-Blind
630      Determination of Methane Detection Limits and Quantification Accuracy Using Aircraft-Based
631      LiDAR. *Elementa: Science of the Anthropocene* **2022**, *10* (1), 00080.
632      https://doi.org/10.1525/elementa.2022.00080.

633 (49) Conrad, B. M.; Tyner, D. R.; Johnson, M. R. Robust Probabilities of Detection and Quantification
634      Uncertainty for Aerial Methane Detection: Examples for Three Airborne Technologies. *Remote*
635      *Sensing of Environment* **2023**, *288*, 113499. https://doi.org/10.1016/j.rse.2023.113499.

636 (50) Bridger Photonics. *Frequently Asked Questions (FAQ)*.
637      https://www.bridgerphotonics.com/methane-detection/frequently-asked-questions-faq (accessed
638      2025-04-29).

639   (51)  Bell, C. S.; Ilonze, C.; Duggan, A.; Zimmerle, D. Performance of Continuous Emission Monitoring
640        Solutions under a Single-Blind Controlled Testing Protocol. *Environ. Sci. Technol.* **2023**, *57* (14),
641        5794–5805. https://doi.org/10.1021/acs.est.2c09235.
642   (52)  Omara, M.; Zimmerman, N.; Sullivan, M. R.; Li, X.; Ellis, A.; Cesa, R.; Subramanian, R.; Presto, A. A.;
643        Robinson, A. L. Methane Emissions from Natural Gas Production Sites in the United States: Data
644        Synthesis and National Estimate. *Environ. Sci. Technol.* **2018**, *52* (21), 12915–12925.
645        https://doi.org/10.1021/acs.est.8b03535.
646   (53)  Pandey, S.; Worden, J.; Cusworth, D. H.; Varon, D. J.; Thill, M. D.; Jacob, D. J.; Bowman, K. W.
647        Relating Multi-Scale Plume Detection and Area Estimates of Methane Emissions: A Theoretical and
648        Empirical Analysis. *Environ. Sci. Technol.* **2025**, *59* (16), 7931–7947.
649        https://doi.org/10.1021/acs.est.4c07415.
650   (54)  Lebel, E. D.; Lu, H. S.; Vielstädte, L.; Kang, M.; Banner, P.; Fischer, M. L.; Jackson, R. B. Methane
651        Emissions from Abandoned Oil and Gas Wells in California. *Environ. Sci. Technol.* **2020**, *54* (22),
652        14617–14626. https://doi.org/10.1021/acs.est.0c05279.
653   (55)  Riddick, S. N.; Mbua, M.; Santos, A.; Emerson, E. W.; Cheptonui, F.; Houlihan, C.; Hodshire, A. L.;
654        Anand, A.; Hartzell, W.; Zimmerle, D. J. Methane Emissions from Abandoned Oil and Gas Wells in
655        Colorado. *Science of The Total Environment* **2024**, *922*, 170990.
656        https://doi.org/10.1016/j.scitotenv.2024.170990.
657   (56)  Townsend-Small, A.; Ferrara, T. W.; Lyon, D. R.; Fries, A. E.; Lamb, B. K. Emissions of Coalbed and
658        Natural Gas Methane from Abandoned Oil and Gas Wells in the United States. *Geophysical*
659        *Research Letters* **2016**, *43* (5), 2283–2290. https://doi.org/10.1002/2015GL067623.
660   (57)  Williams, J. P.; Regehr, A.; Kang, M. Methane Emissions from Abandoned Oil and Gas Wells in
661        Canada and the United States. *Environ. Sci. Technol.* **2021**, *55* (1), 563–570.
662        https://doi.org/10.1021/acs.est.0c04265.
663   (58)  Lyon, D. R.; Alvarez, R. A.; Zavala-Araiza, D.; Brandt, A. R.; Jackson, R. B.; Hamburg, S. P. Aerial
664        Surveys of Elevated Hydrocarbon Emissions from Oil and Gas Production Sites. *Environ. Sci.*
665        *Technol.* **2016**, *50* (9), 4877–4886. https://doi.org/10.1021/acs.est.6b00705.
666   (59)  Hmiel, B.; Lyon, D. R.; Warren, J. D.; Yu, J.; Cusworth, D. H.; Duren, R. M.; Hamburg, S. P. Empirical
667        Quantification of Methane Emission Intensity from Oil and Gas Producers in the Permian Basin.
668        *Environ. Res. Lett.* **2023**, *18* (2), 024029. https://doi.org/10.1088/1748-9326/acb27e.
669   (60)  Lyman, S. N.; Tran, T.; Mansfield, M. L.; Ravikumar, A. P. Aerial and Ground-Based Optical Gas
670        Imaging Survey of Uinta Basin Oil and Gas Wells. *Elementa: Science of the Anthropocene* **2019**, *7*,
671        43. https://doi.org/10.1525/elementa.381.
672   (61)  Daniels, W. S.; Jia, M.; Hammerling, D. M. Estimating Methane Emission Durations Using
673        Continuous Monitoring Systems. *Environ. Sci. Technol. Lett.* **2024**, *11* (11), 1187–1192.
674        https://doi.org/10.1021/acs.estlett.4c00687.
675   (62)  Chen, Q.; Schissel, C.; Kimura, Y.; McGaughey, G.; McDonald-Buller, E.; Allen, D. T. Assessing
676        Detection Efficiencies for Continuous Methane Emission Monitoring Systems at Oil and Gas
677        Production Sites. *Environ. Sci. Technol.* **2023**, *57* (4), 1788–1796.
678        https://doi.org/10.1021/acs.est.2c06990.
679   (63)  Chen, Y.; Sherwin, E. D.; Berman, E. S. F.; Jones, B. B.; Gordon, M. P.; Wetherley, E. B.; Kort, E. A.;
680        Brandt, A. R. Quantifying Regional Methane Emissions in the New Mexico Permian Basin with a
681        Comprehensive Aerial Survey. *Environ. Sci. Technol.* **2022**, *56* (7), 4317–4323.
682        https://doi.org/10.1021/acs.est.1c06458.
683   (64)  Schissel, C.; Allen, D. T. Impact of the High-Emission Event Duration and Sampling Frequency on the
684        Uncertainty in Emission Estimates. *Environ. Sci. Technol. Lett.* **2022**, *9* (12), 1063–1067.
685        https://doi.org/10.1021/acs.estlett.2c00731.

686     (65)   Day, R. E.; Emerson, E.; Bell, C.; Zimmerle, D. Point Sensor Networks Struggle to Detect and
687            Quantify Short Controlled Releases at Oil and Gas Sites. *Sensors* **2024**, *24* (8), 2419.
688            https://doi.org/10.3390/s24082419.
689     (66)   Cheptonui, F.; Emerson, E.; Ilonze, C.; Day, R.; Levin, E.; Fleischmann, D.; Brouwer, R.; Zimmerle, D.
690            Assessing the Performance of Emerging and Existing Continuous Monitoring Solutions under a
691            Single-Blind Controlled Testing Protocol. ChemRxiv April 29, 2025.
692            https://doi.org/10.26434/chemrxiv-2024-f1znb-v2.
693

694

695 # Supporting Information for:

696 # Extrapolation Approaches for Creating

697 # Comprehensive Measurement-Based Methane

698 # Emissions Inventories

699 *Bailey K. Fosdick[1], Zachary Weller[1], Hon Xing Wong[1], Abigail Corbett[1], Yannik Roell[1], Ella*

700 *Martinez[1], Amanda Berry[1], Natalia Gielczowski[1], Kristian D. Hajny[1], Christopher Moore[1]*

701 [1] GTI Energy

702

703

704

705 This document contains 6 pages with 2 text sections (Text S1 – S2), 3 figures (Figure S1 – S3),

706 and 1 table (Table S1)

707
708

709

## Text S1. Anonymization Method

710

711     The anonymized data used in this work are noised versions of real data collected in 2023 from

712 a dry-gas basin that has been shared by our operator partners. To anonymize the data, we assign

713 each site a randomly selected scaling factor drawn from a common distribution. Individual data

714 values (e.g. point sensor network (PSN), aerial, production) are then multiplied by a randomly

715 generated datapoint-specific scaling factor closely centered around the site-specific value in a way

716 that allows individual data values to be increased or decreased. This preserves important features

717 (e.g., missing values, skewed distribution) and relationships (e.g., temporal correlation) while

718 making the true values unrecoverable by a third party.

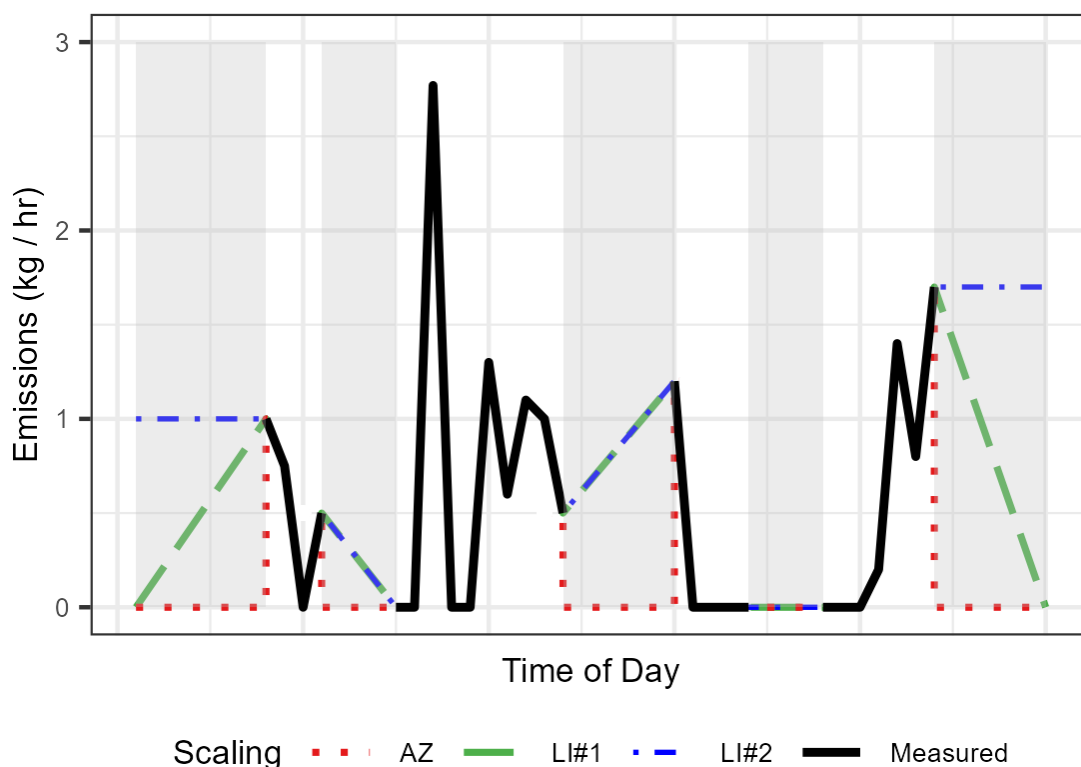## Text S2. Linear Temporal Extrapolation

719

720     The main text discusses using linear interpolation for periods of no information. If there is a

721 period of no information at the beginning or end of the dataset (not including unmonitored periods),

722 then there are not two data points to interpolate between. This was handled by extrapolating the

723 measured endpoint throughout this period of no information as a constant. An alternative was

724 tested where the missing endpoint is assumed to be zero. Although these approaches could result

725 in significantly different results in some cases, for the randomly selected 50 sites, the difference in

726 the total emissions was minimal (without accounting for unmonitored months, PSN A data: 108

727 MT $CH_4$ vs 109 MT $CH_4$; PSN B data: 342 MT $CH_4$ vs 342 MT $CH_4$).

728

729
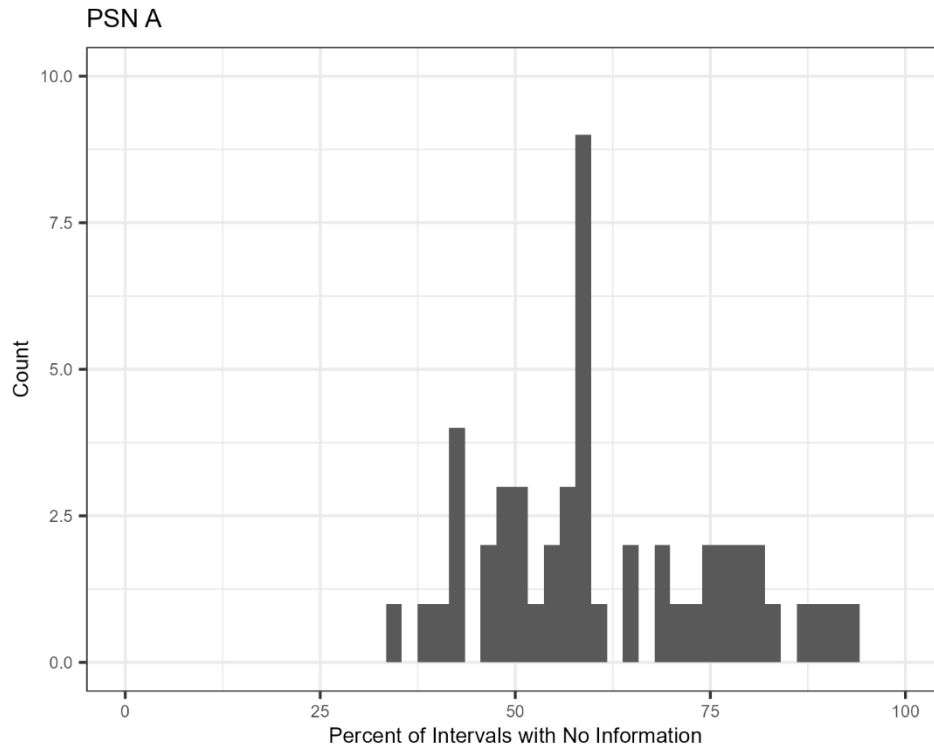
730 **Figure S1.** Percentage of 15-minute intervals with emission rate originally reported as missing

731 (period of no information) for sites monitored by PSN A.

732
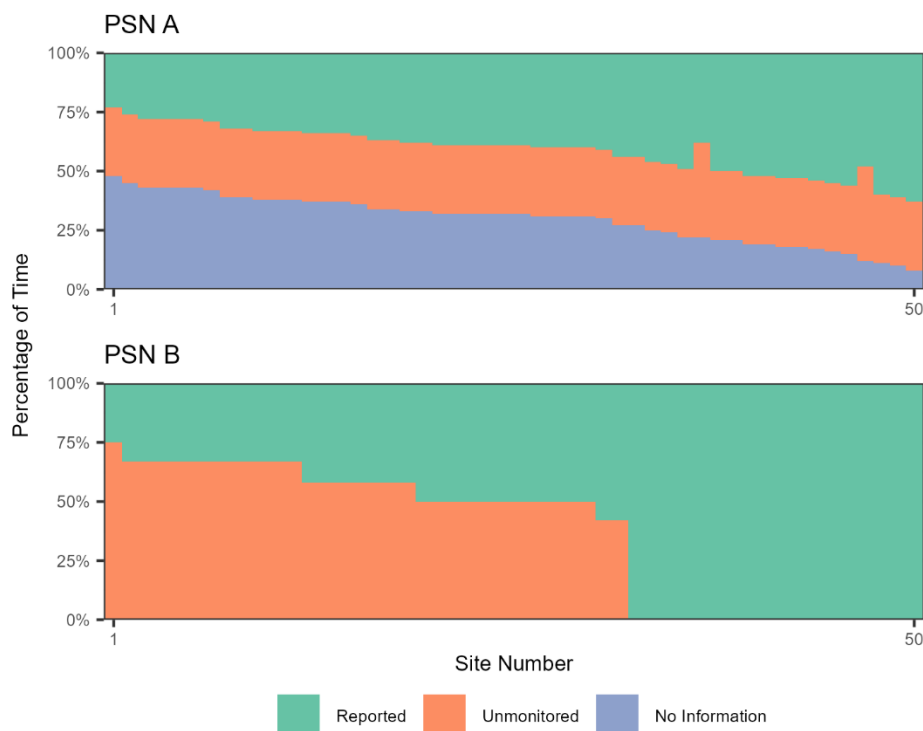
733    **Figure S2.** Percentage of time during 2023 for each site when the site was unmonitored, there was

734    a period of no information, and the PSN reported an emission rate. Based on the originally reported

735    data.

736

737     **Figure S3.** Temporal extrapolation methods applied to simulated data, with five periods of no

738     information (denoted by the grey bands) used to illustrate the effects of the different methods. The

739     measured data is denoted in black. The extrapolation methods shown include assuming all

740     emission rates during periods of no information are zero (AZ = all zero; red),linear interpolation

741     between observed emission rates on either side of the period of no information and assuming

742     missing endpoints are zero (LI#1 = linear interpolation method 1; green), and extrapolating a

743     constant on the boundary period of no information (LI#2 = linear interpolation method 1; blue).

744     The naïve scaling methods (2 and 3) are not shown as they are performed on the aggregate total

745     emissions.

746

747  **Table S1.** Site characteristics for those with PSN and those without PSN. Production is reported

748  in barrels of oil equivalent per day (BOED).

| Site Characteristic | PSN A (50) | PSN B (50) | Unmonitored (100) |
|---|---|---|---|
| **GHGRP Reported Emissions (Tonnes CH$_4$)** | | | |
| % reported as zero | 24% | 4% | 19% |
| Median emissions (w/o zeros) | 1.1 | 3.0 | 1.2 |
| **Production (BOED)** | | | |
| % reported as zero | 4% | 0% | 5% |
| Median production (w/o zero) | 1253 | 1335 | 119 |
| **Production Strata (%)** | | | |
| Inactive/No Data (0 BOED or NA) | 4% | 0% | 5% |
| Marginal (1-15 BOED) | 12% | 0% | 40% |
| Standard (16-300 BOED) | 48% | 60% | 53% |
| High (>300 BOED) | 36% | 40% | 2% |
| **Age (Years)** | | | |
| Median age | 10 | 6 | 13 |
| **PSN Emissions (Tonnes CH$_4$)** | | | |
| Median annual emissions | 0.2 | 0.3 | NA |

749

750